Desalination and Water Treatment
www.deswater.com

doi: 10.5004/dwt.2023.29374

289 (2023) 238–247
March

Evaluating the efficiency of scallop shell/iron oxide(II) nanocomposite in removal of Direct red 81 dye from aqueous solutions: kinetic, isotherm and thermodynamic studies

Khadijeh Dadras[a], Seyed Davoud Ashrafi[b], Kamran Taghavi[a,*], Jalil Jaafari[b,*]

[a]*Department of Environmental Health Engineering, School of Health, Guilan University of Medical Sciences, Rasht, Iran, Tel.: +98 131 3229599; Fax: +98 131 3234155; emails: k.taghavi@gums.ac.ir (K. Taghavi), dadras_khadije@yahoo.com (K. Dadras)*
[b]*Research Center of Health and Environment, Department of Environmental Health Engineering, School of Health, Guilan University of Medical Sciences, Rasht, Iran, Tel.: +98 131 3229599; Fax: +98 131 3234155; emails: jalil.jaafari@yahoo.com (J. Jaafari), d_ashrafi@yahoo.com (S.D. Ashrafi)*

Received 28 October 2022; Accepted 17 February 2023

ABSTRACT

These dyes have the potential for mutagenicity, carcinogenicity, and unwanted color on the one hand, and on the other hand, cause the production of toxic by-products in aqueous media. The aim of the present work is to synthesize scallop shell/iron oxide(II) nanocomposite and evaluate its efficiency in removing Direct red 81 (DR81) dye from aqueous solutions. Iron oxide nanoparticles were prepared by co-precipitation method and then the scallop was coated with iron oxide. The properties of synthesized nanocomposite were identified using Fourier-transform infrared spectroscopy, field-emission scanning electron microscopy, and X-ray diffraction. Effect of dye concentration (20–120 mg/L), contact time (0–240 min), adsorbent dosage (0.5–2.5 g), pH (3–11), and temperature (25°C–55°C) was investigated on decolorization efficiency of the process. Under optimal conditions (an initial DR81 concentration of 25 mg/L, pH of 3, adsorbent dose of 0.5 g, and contact time of 90), more than 98% of the dye was removed. The results showed that the efficiency decreases with increasing concentration. Moreover, by increasing the contact time and adsorbent dosage, dye adsorption percentage was enhanced. The maximum adsorption coefficient was 46.4 mg/g. In addition, Freundlich and Langmuir models were used to analyze the experimental isotherm data. The kinetic data of the adsorption process were in good agreement with the pseudo-second-order kinetic model (0.995). The experimental data of the adsorption process followed the Langmuir model (R^2 = 0.91). The results show that Fe_2O_3 nanoparticles coated with scallop shell as an environmentally friendly adsorbent can be effective in the adsorption of DR81.

Keywords: Adsorption; Iron oxide; Scallop shell; Direct red 81 dye

1. Introduction

Water, as the most vital human need, is of great economic, social, political, and environmental importance in the world [1–3]. Population growth, industrial development, and production of industrial effluents along with climate change cause a quantitative and qualitative decline in water resources available to humans and introduce a variety of pollutants into aquatic environments [4,5]. Therefore, in order to reuse water, it is necessary to treat the contaminated water sources. The presence of colorful organic matter in water resources is one of the most important environmental challenges in the world today. Most dyes are toxic, carcinogenic, and mutagenic, so it is important to remove the dye from contaminated water samples [6]. Industrial effluents from textile and dyeing industries, pulp and paper production, food industry, and chemical production may

* Corresponding authors.

1944-3994/1944-3986 © 2023 Desalination Publications. All rights reserved.

enter dyes to natural streams and rivers [7]. Direct red 81 dye (DR81) belongs to the azo dye family, which is used for dyeing silk, wool, and nylon fibers. It is also used as an indicator in complexometric titration to measure calcium, magnesium, zinc ions, and bio-pigments [8]. This dye is known as a highly toxic compound because when it decomposes in water, it forms a highly carcinogenic compound called naphthoquinone [9]. Among the various methods available for the removal of dyes and other organic compounds from contaminated water, the adsorption method using inexpensive adsorbents is considered [6,10,11]. The surface characteristics and functional groups are very important in the performance of different types of adsorbents in removing contaminants.

Numerous studies have been performed to remove DR81 from aqueous solutions, such as the use of tree bark, carbon obtained from rice husk [12], sawdust [9], potato husk, or the use of reverse osmosis [13] and electrocoagulation [14]. However, most of these methods, except for the use of adsorbents, are ineffective when the contaminant concentration is low and have disadvantages such as the high cost associated with the employment of equipment and processes, sludge production or other toxic wastes as well as the need for energy and large space [15–20]. Membrane processes are also costly and their management requires specialized personnel. Oxidation–reduction also requires the addition of extra chemicals to the wastewater, which in turn causes secondary pollution in the environment [21]. The scallop is a bivalve mollusc belonging to the *Pectinidae* family. Scallops are found in the oceans and seas all over the world. Due to their abundance in nature, scallops are economically viable [22] and lead to fewer iron particles to be used, thus saving costs. The magnetic property of the adsorbent, in addition to the advantages mentioned above, lead to easy separation using a magnet [23] because the separation of the scallop is very difficult due to its small particle size and the combination of these two materials in the form of nanocomposites is very useful and efficient and leads to an increase in the adsorption of contaminants [24]. Due to the fact that so far, no studies have been performed for the adsorption of dyes, including DR81 with scallop shell/iron oxide nanocomposite, therefore, the aim of this study was to prepare the scallop shell/iron oxide nanocomposite for adsorption of DR81 from aqueous medium. In this study, effective parameters in the adsorption process such as pH, contact time, adsorbent dosage, contaminant concentration, and process temperature as well as prepared adsorbent properties were investigated, and isotherms, kinetics, and thermodynamics of adsorption were studied.

2. Materials and methods

2.1. Chemicals

This is a basic-applied study in which the performance of magnetized powdered activated carbon with iron oxide nanoparticles as an adsorbent in the adsorption of Direct red dye 81 was investigated on the experimental pilot scale. In the present study, DR81 was selected as an azo dye; it was purchased from Alvan Sabet Company, Hamedan, and other required chemicals such as $FeCl_2{\cdot}4H_2O$, $FeCl_3{\cdot}6H_2O$, HCl, NaOH, CO_2Na_3, and ethanol (96%) were purchased from Merck Company, Germany. The magnet was also used to separate the magnetic sorbent from the solution. Fig. 1 shows the chemical structure of DR81 [25].

2.2. Preparation of calcined scallop shell

Scallop shells were collected from the shores of the Caspian Sea in Gilan Province and washed several times with distilled water to remove dust and impurities. Then, for easier use, they were milled using a hammer mill. Lastly, they were dried in an electric oven at 1,000°C for 5 h and finally sieved with ASTM standard sieve No.50. Table 1 lists the chemical composition of the scallop shell. Fig. 2 shows the raw scallop and its powder.

2.3. Synthesis of nanocomposites

1.98 g of calcined scallop, 1.98 g of $FeCl_2$, and 5.406 g of $FeCl_3$ were added to 80 mL of solution containing pure ethanol (96%) and 20 mL of deionized water, mixed and stirred with a magnetic stirrer for 30 min, then refluxed. Then, reflux was performed at 80°C for 1 h. Afterward, by adding 20 mL of ammonium hydroxide and continuing reflux, a bitumen solution was finally obtained after 2 h of synthesis, and after washing with deionized water and ethanol,

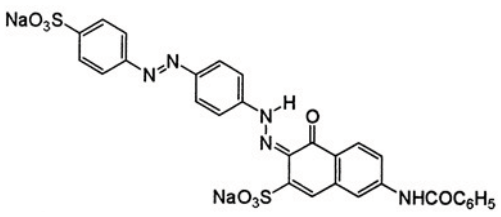

Fig. 1. Structure of Direct red 81 dye.

Table 1
Chemical composition of scallop shell

CaO (%)	58.45
Na (%)	0.52
MgO (%)	0.25
P_2O_5 (%)	0.08
K_2O (%)	0.019
Fe (mg/kg)	65.8
Mn (mg/kg)	4.3
Cu (mg/kg)	4.2
Zn (mg/kg)	3.1

Fig. 2. Scallop shell and its powder.

the particles were separated by a magnet and dried at room temperature [26]. By heating the sample for several hours at a temperature above 150°C, the color change from bitumen to reddish-brown indicates the formation of γ-Fe_2O_3, which can be proved by X-ray analysis. It should be noted that the synthesis of γ-Fe_2O_3 was performed without the presence of scallops to ensure the correct synthesis. Thereafter, the synthesis of nanocomposite was performed. X-ray diffraction (XRD) analysis was used to determine the type of nanoparticle; field-emission scanning electron microscopy was employed to determine the particle size, and Fourier-transform infrared spectroscopy (FTIR) was performed on the powdered samples.

2.4. Adsorption experiments

After preparation of scallop shell/iron oxide(II) nanocomposite, preparation of DR81 stock solution with a concentration of 1,000 mg/L was done, and adsorption studies were performed in several sections with deionized water. First, aqueous solutions with a volume of 100 mL containing DR81 with different concentrations (10, 25, 50, 75, and 100 mg/L) were prepared. The pH of the solutions was then adjusted to the initial pH values of 3, 5, 7, 9, and 11 using 0.01 M hydrochloric acid and sodium hydroxide solutions. 0.1–1.5 g of adsorbent was added to each solution separately. The samples were then placed on a shaker at 150 rpm. After the desired time (10–240 min), the solution was sampled. For complete separation of the solid phase (adsorbent) from the liquid phase of all samples, a 45 μm filter was used under vacuum pump suction. All experiments were repeated twice and their mean was presented as the final result. A spectrophotometer was used to draw the calibration curve and measure the final DR81 after the process. After determining the final concentration, to calculate the percentage of adsorption, Eq. (1) was employed, and the adsorption capacity was calculated by Eq. (2) [27,28]:

$$R = \left(\frac{C_0 - C_e}{C_0} \right) \tag{1}$$

$$q_e = \frac{C_0 - C_e}{m} \times V \tag{2}$$

where the q_e is adsorption capacity (g/mg); C_0 is initial concentration of solution (mg/L); C_e is final concentration after equilibration (mg/L); V is volume of liquid inside the reactor (L), and M is adsorbent mass (g) [29,30].

The point of zero charge (pH_{pzc}) were used to characterize the surface charge changes of adsorbents. To determine the pH_{pzc} point, 100 mL of 0.01 M potassium nitrate was added to glass containers. Then, the pH of the initial solution was adjusted in the range of 2–12 by 0.01 M hydrochloric acid and sodium hydroxide. After that, 0.5 g of adsorbent was added to each of the desired containers and stirred for 48 h. After this time, the solutions were filtered by a 45 μm Whatman Filter, and their pH was finally measured.

2.5. Determination of adsorption isotherms

The Langmuir isotherm model is valid in terms of monolayer adsorption. The linear form of Langmuir isotherm model is given in Eq. (3).

$$\frac{C_e}{q_e} = \frac{C_e}{q_m} + \frac{1}{b \times q_m} \tag{3}$$

where q_e is the amount of the adsorbed substance per mass unit of the absorbent in equilibrium (mg/g), C_e is the equilibrium concentration of the adsorbed substance in a solution after adsorption (mg/L), q_m is the maximum amount of the adsorbed substance per mass unit for the adsorbent at equilibrium (mg/g) and b is the Langmuir constant.

The linear form of Freundlich isotherm model is given in Eq. (4) [31]:

$$\log q_e = \log K_f + \frac{1}{n} \log C_e \tag{4}$$

where q_e is the amount of the substance adsorbed per mass unit at equilibrium (mg/g), C_e is the equilibrium concentration of the adsorbed substance in the solution after adsorption (mg/L), and K_f and n are Freundlich constants.

Important parameters, which should be determined in the adsorption equations to predict the suitability or non-suitability of adsorption and the type of adsorption process are the dimensionless coefficient of R_L and the n coefficient, which are obtained from the Langmuir and Freundlich equations, respectively. The R_L equilibrium parameter is defined as Eq. (5) [32]:

$$R_L = \frac{1}{1 + bC_0} \tag{5}$$

where b is Langmuir constant and C_0 is the initial DR81 concentration. The R_L value indicates the type of isotherm as follows: irreversible adsorption for $R_L = 0$, optimal adsorption for $0 < R_L < 1$, linear adsorption for $R_L = 1$ and undesirable adsorption for $R_L > 1$. In Freundlich equation, $1/n$ with values from 0 to 1 indicates surface heterogeneity. A value of $1/n < 1$ indicates that the DR81 adsorption on the adsorbent is better at lower concentrations, and the results obtained in this study indicate the same result [33,34].

2.6. Adsorption kinetics

One of the most important factors for designing the adsorption system to determine the contact time and obtain the dimensions of the discontinuous reactor is the anticipation of the speed of the adsorption process that is controlled by the kinetics of the system. In order to study the mechanism of adsorption, adsorption constants can be calculated using Eq. (6), that is, Lagergren model Lagergren (pseudo-first-order kinetic) and Eq. (7), that is, Ho model (pseudo-second-order kinetic) [33,35].

$$\log\left(q_e - q_t\right) = \log q_e - k_1 t \tag{6}$$

$$\frac{t}{q_t} = \frac{1}{q_e^2 k_2} + \frac{1}{q_e} t \quad (7)$$

In Eq. (6) q_e is the amount of substance absorbed at equilibrium (mg/g), q_t is the amount of substance absorbed at time t (mg/g) and k_1 is constant rate of pseudo-first-order kinetic (min^{-1}). In Eq. (7) q_e is the amount of material absorbed at equilibrium (mg/g) and k_2 is constant rate of pseudo-second-order kinetic (g/mg·min).

3. Results and discussion

3.1. Identification of surface properties of scallop shell/iron oxide(II) nanocomposite

Fig. 3 shows the FTIR image scallop shell/iron oxide(II) nanocomposite to identify and investigate the functional groups present on the adsorbent surface. These functional groups are one of the reasons for the adsorption process or an obstacle to doing so [35]. Fig. 4 shows the XRD image of the scallop shell/iron oxide(II) nanocomposite. As shown, Fig. 4a shows that the peaks appearing are not wide. It can be concluded that nanoparticles are crystalline, and there is an interaction between scallop and iron oxide(II) nanocomposite (Fig. 4b).

FTIR spectra are a very important way to determine the characteristics of functional groups and to study the changes in these groups in the adsorbent. FTIR spectrum of scallop shell/iron oxide nanocomposite (II) is shown in Fig. 3. As the results showed, the range of 400–4,000 cm^{-1} is related to the minerals in scallop shell/iron oxide(II) nanocomposite such as carbonate, phosphate, sulfate and nitrate, phosphate, carbonyl, and nitrate. The scallop shell/iron oxide(II) nanocomposite contains various functional groups such as amines, alcohols, carbonyls, and hydroxyl [36]. The spectrum of 3,200–3,600 cm^{-1} is related to the stretching zone of functional groups of H–O and H–N (35); the spectrum of 2,400–2,950 cm^{-1} is ascribed to the stretching zone of H–C, and peaks in the range of 2,999–3,449 cm^{-1} belong to the functional groups of hydroxyl and amine [37]. Also, peaks at 2,196 and 2,928 cm^{-1} indicate the presence of the H–C group, and two peaks 1,594 and 1,655 cm^{-1} indicate the presence of amine functional group. Obtained results was confirmed by similar study which use scallop shell coated Fe_2O_3 for adsorption of tetracycline [23]. The peak at 1,649 cm^{-1} proves the presence of the carbonyl group on the surface of the scallop shell/iron oxide(II) nanocomposite. According to the results, the presence of shifts and shortening and widening of the peaks after the adsorption process represents the presence of DR81 on the scallop shell/iron oxide(II) nanocomposite [38].

In order to evaluate the morphological and surface characteristics of iron oxide and scallop shell/iron oxide(II) nanocomposite, scanning electron microscopy analysis was used. Figs. 1–3 show the morphological studies of scallop shell/iron oxide(II) nanocomposite. These figures confirmed the surface of scallop shell/iron oxide(II) nanocomposite confirmed the crystal structure of both types. Fe_2O_3 coating was also present on the scallop, as shown in Fig. 3. The average size of scallop shell/iron oxide(II) nanocomposite was around 26 nm. Peaks were correspondent to the values of 18.07, 19.12, 20.17, 24.05, 37.31, 37.58, 43.29, 54.38, 56.38, 56.07, 56.49, and 78.49 and 7.49, 7.49, and 56.49. Scallop shell/iron oxide(II) nanocomposite showed that the nanocomposites are single-phase with a quadrilateral structure. A comparison of the XRD patterns presented is shown in Fig. 2. After that, the state of iron capacity was almost unchanged. Various studies show that the porous and layered structure of adsorbent and scallop shell/iron oxide(II) nanocomposite developed the contact surface and increased the adsorption of dye ions into the adsorbent, which plays an important role in the ability to adsorb [23].

3.2. Effect of pH on the DR81 removal by scallop shell/iron oxide(II) nanocomposite

The pH of the solution is one of the important control parameters in the adsorption process. The results of the

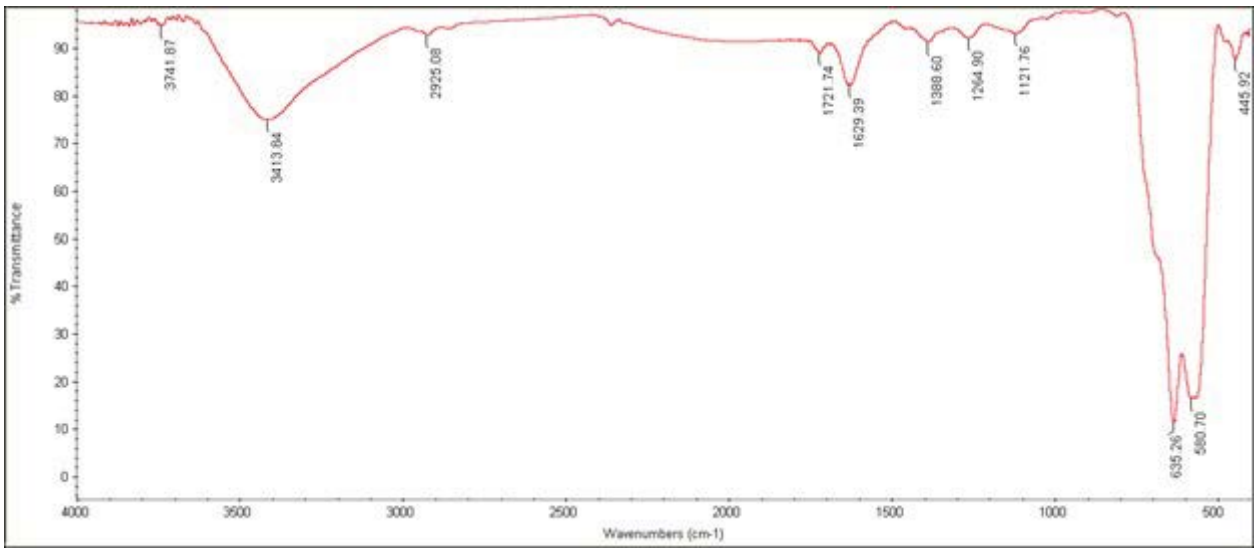

Fig. 3. Fourier-transform infrared spectrum of scallop shell/iron oxide(II) nanocomposite.

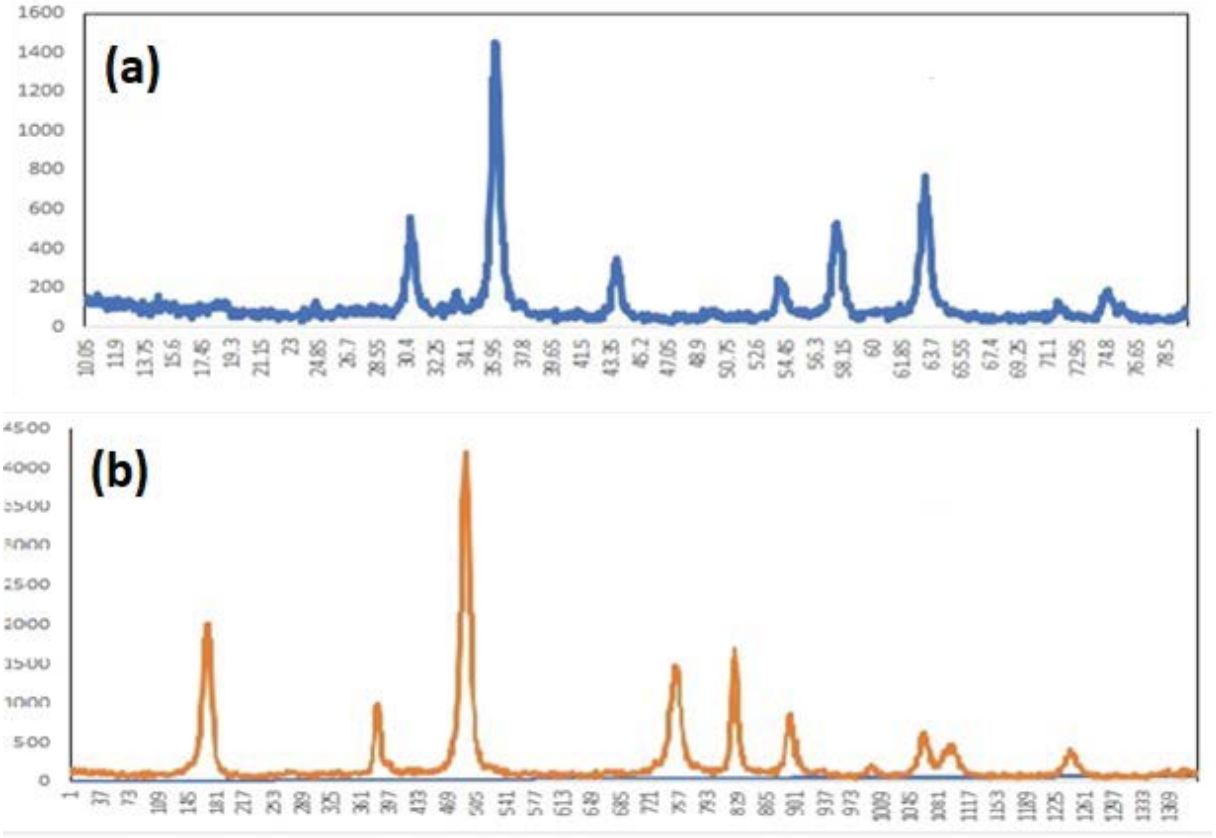

Fig. 4. X-ray diffraction pattern of scallop shell/iron oxide(II) nanocomposite.

effect of different pH values on the DR81 adsorption by scallop shell/iron oxide(II) nanocomposite are shown in Fig. 5. By increasing the pH to values higher than this value, the efficiency of the adsorption process decreased. Therefore, a pH of 3 was considered as the optimal pH.

In the adsorption process, the pH of the solution plays a very important role in the adsorption capacity and surface charge of the adsorbent, so that it affects the adsorbent surface characteristics, the functional groups on the active sites, the degree of ionization, and the removal efficiency. pH ionizes the materials in the solution and separates the functional groups present on the active sites of the scallop shell/iron oxide nanocomposite (II). The results of this study showed that with changes in pH from 3 to 11, the efficiency of scallop shell/iron oxide nanocomposite (II) decreased so that at pH of 3, the highest adsorption efficiency (98%) was obtained. The main factor of DR81 adsorption on scallop shell/iron oxide nanocomposite (II) is active sites and functional groups on the cell wall of scallop shell/iron oxide nanocomposite (II). There is a protein on the cell wall of scallop shell/iron oxide nanocomposite (II) that contains functional groups of amines. Amines are protonated at acidic pH values and their electrostatic charge gets positive [39], which causes adsorption of DR81 on scallop shell/iron oxide nanocomposite (II). Fig. 1 shows that the highest amount of DR81 adsorption was observed at a pH of 3; thus, a pH of 3 was selected as the optimal pH. In the study conducted by Ashrafi et al. [10], DR81 dye removal was performed

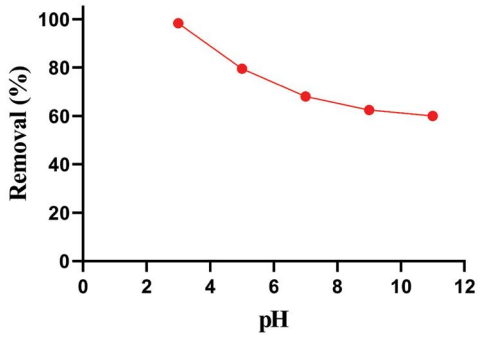

Fig. 5. Effect of pH on Direct red 81 adsorption on adsorbent (dye concentration of 25 mg/L, amount of adsorbent 0.5 g and contact time of 90 min).

using modified rice husk/NaOH. The highest adsorption efficiency (95%) for initial dye concentration of 25 mg/L and adsorbent dosage of 6 g/L was obtained at pH 5. It has a significant effect on the adsorption process, so the effect of pH can be depending on the type of pollutant and specific adsorbent. In general, based on the results of this study and other studies, it can be said that pH has a significant effect on the removal of contaminants using the adsorption process. Therefore, the effect of pH can depend on the type of pollutant and specific adsorbent. By measuring the pH_{zpc} of scallop shell/iron oxide nanocomposite (II), its value was

6.31, which means that the electrostatic charge of the solution at pH less than pH_{zpc} is positive while it is negative at the pH values more than pH_{zpc} [35]. Depending on the type of pollutant, better adsorption occurs at pH less than pH_{zpc}. Another reason for the highest adsorption at a pH of 6 could be the deformation of scallop shell/iron oxide nanocomposite (II) at other pH values. In fact, the highest strength of the cell wall structure of scallop shell/iron oxide nanocomposite (II) is a pH of 6 and its structure is decomposed at other pH values. The results of this study are consistent with studies conducted by Fakhri [40] and Vadi et al. [41].

3.3. Effect of time on the dye removal by nanocomposites

The results of the effect of contact time on the absorption of DR81 are shown in Fig. 6. In this study, the amount of 0.5 g of scallop shell/iron oxide(II) nanocomposite in 100 mL dye solution (25 mg/L) was examined at a pH of 5 and a time range of 10–120 min. The results showed that with increasing the contact time, the DR81 adsorption efficiency also increased. This increase in adsorption was done rapidly up to 90 min. However, after this time up to 90 min, there was no significant increase in adsorption. In fact, the DR81 adsorption reached equilibrium, and after 120 min, desorption was observed.

Contact time is one of the factors affecting the adsorption process. The adsorption percentage of DR81 by scallop shell/iron oxide(II) nanocomposite was directly related to the contact time, so that with increasing the contact time from 10 to 90 min, the adsorption efficiency increased. At the beginning of the adsorption reaction, due to the frequency of adsorption sites and the large difference between the concentration of adsorbent in the solution and its amount on the surface of scallop shell/iron oxide(II) nanocomposite, the removal percentage increased. It is also difficult to occupy the remaining empty surface sites over time, because there is a kind of repulsion between the molecules adsorbed on the adsorbent surface and the molecules in the solution phase. As the results showed, in the first 90 min, about 70% was removed by scallop shell/iron oxide(II) nanocomposite. According to the experimental results, it is observed that the adsorption value for scallop shell/iron oxide(II) nanocomposite does not change much after 90 min. In this case, the amount of DR81 absorbed on the surface of the scallop shell/iron oxide(II) nanocomposite will be equal to the amount of DR81 present in the solution phase. Therefore, the contact time of 90 min was obtained as the equilibrium time. It is consistent with the results of Khan et al. [42] and Dehghani et al. [39]. In the study conducted by Khan et al. [42], kaolin coated with magnesium oxide was used to remove DR81 from aqueous solutions. The highest amount of DR81 removal was obtained during a contact time of 90 min [42].

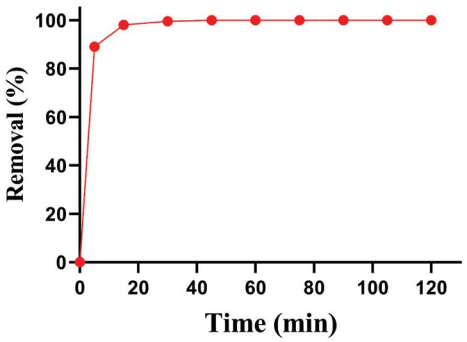

Fig. 6. Effect of contact time on Direct red 81 adsorption (dye concentration of 25 mg/L, adsorbent dosage of 0.5 g, and pH of 3).

3.4. Effect of adsorbent on dye removal by scallop shell/iron oxide(II) nanocomposite

At this stage, to determine the optimal adsorbent dosage, according to previous studies, the values of 0.25–1.5 g/L of scallop shell/iron oxide(II) nanocomposite were added to a dye solution of 25 mg/L at an optimal pH of 3, and after 90 min of mixing, DR81 dye adsorption of onto scallop shell/iron oxide(II) nanocomposite was investigated. According to Fig. 7, the maximum adsorption capacity of DR81 by scallop shell/iron oxide nanocomposite (II) was 12.28.

In this study, it was observed that by increasing the amount of scallop shell/iron oxide(II) nanoparticles, the process efficiency also increased. In other words, by increasing the amount of scallop shell/iron oxide(II) nanoparticles from 0.25 to 1.5 g/L, the DR81 removal efficiency increased from 30% to 79%. In describing this fact, it can be stated that with increasing the amount of scallop shell/iron oxide(II) nanocomposite, the available and active adsorption sites for interactions between scallop shell/iron oxide(II) nanocomposite and DR81 were increased [43]. When the dose of scallop shell/iron oxide(II) nanocomposite reached 1.5 g/L, the adsorption percentage increased to 79%. Also, the maximum adsorption capacity of DR81 by scallop shell/iron oxide(II) nanocomposite was 46.29%; this increase in dye adsorption can be due to increased contact surface area of scallop shell/iron oxide(II) nanocomposite followed by an increase in active sites that cause adsorption DR81 on scallop shell/iron oxide(II) nanocomposite. However, scallop shell/iron oxide(II) nanocomposite reduces the adsorption capacity due to the unsaturation of the active sites of scallop shell/iron oxide(II) nanocomposite during the adsorption process [44]. Removal of DR81 had a good rate up to the scallop shell/iron oxide(II) nanocomposite dosage of 0.75 g and the adsorption rate was not significantly increased after this amount; thus, to reduce costs, 0.75 g of nanocomposite was considered as the optimal dosage. This was consistent

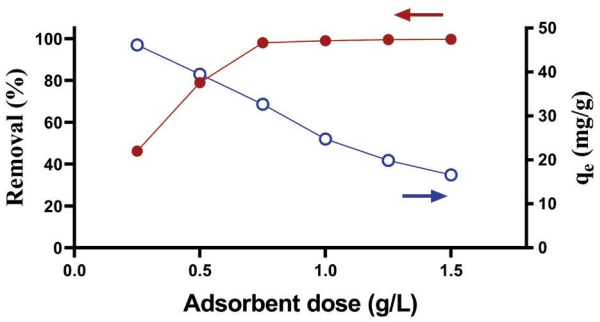

Fig. 7. Effect of adsorbent on Direct red 81 (dye concentration 25 mg/L, optimal pH of 3, and contact time of 90 min).

with the study of Zang et al. [45]. Also, these findings are consistent with the results of the study of Shojaei et al. [46] who studied the adsorption of DR81 by zero-valent iron nanoparticles; so that they concluded that by increasing the adsorbent dose from 0.9 to 9 g/L, the dye removal efficiency increases rapidly 65% to 97%.

3.5. Effect of initial dye concentration on the dye adsorption by scallop shell/iron oxide(II) nanocomposite

To evaluate the optimal concentration in the removal of DR81, the optimal values obtained in the previous steps were tested at dye concentrations of 10–100 mg/L, and the results were presented in Fig. 8. As shown by the results, with increasing the initial DR81 concentration, its adsorption decreased. The highest adsorption efficiency (98%) was obtained at a dye concentration of 25 mg/L and a contact time of 80 min and a pH of 3. The maximum adsorption capacity of DR81 by scallop shell/iron oxide(II) nanocomposite was 12.25. In Fig. 9, the effect of the initial DR81 concentration on its adsorption efficiency was investigated. As shown in the figure, with increasing the initial concentration of DR81, the adsorption efficiencies decreased. The maximum DR81 adsorption efficiency was obtained at a concentration of 10 mg/L. The percentage of DR81 removal for initial concentration of 10 mg/L was 78%, which was reduced to 37% for the DR81 concentration of 30 mg/L. The reason for the decrease in adsorption can be explained by the fact that with increasing the concentration of the contaminant, the residual amount increases and reduces the efficiency. Also, in high concentrations, the adsorbent surface is saturated and reduces the adsorption of dye. The maximum adsorption capacity of DR81 by iron oxide nanoparticles coated with the scallop was 12.28. The increase in adsorption capacity can be also justified by the increase in repulsive force due to the increase in concentration gradient, which is consistent with the study of Arami et al. [47].

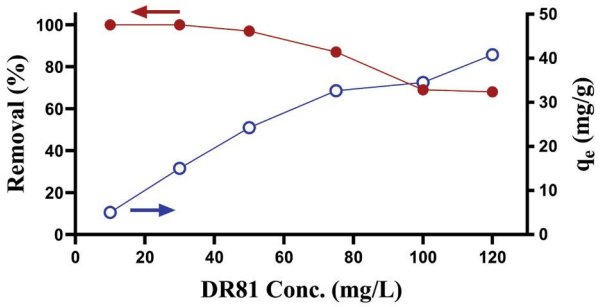

Fig. 8. Effect of Direct red 81 concentration (adsorbent dosage of 0.5 g/L, optimal pH of 3, and contact time of 80 min).

3.6. Isotherm studies of DR81 adsorption

Table 2 shows the adsorption isotherms and theoretical parameters of the models along with the regression coefficients related to the dye adsorption by the scallop shell/iron oxide(II) nanocomposite. According to the regression value (R^2) obtained for each of the isotherms, it is observed that the Langmuir model (R^2 = 0.903) has the highest value and the best model used in the adsorption of dye by the adsorbent. Therefore, it can be concluded that the adsorbent surface is homogeneous and the adsorption is mainly monolayer.

Table 2
Results obtained from the calculations of Direct red 81 adsorption isotherms

Freundlich isotherm			Langmuir isotherm			
R^2	K_f (mg/g)	1/*n*	R^2	q_m (mg/g)	K_L (L/mg)	R_L
0.917	25.71	0.182	0.996	46.3	3.58	0.01

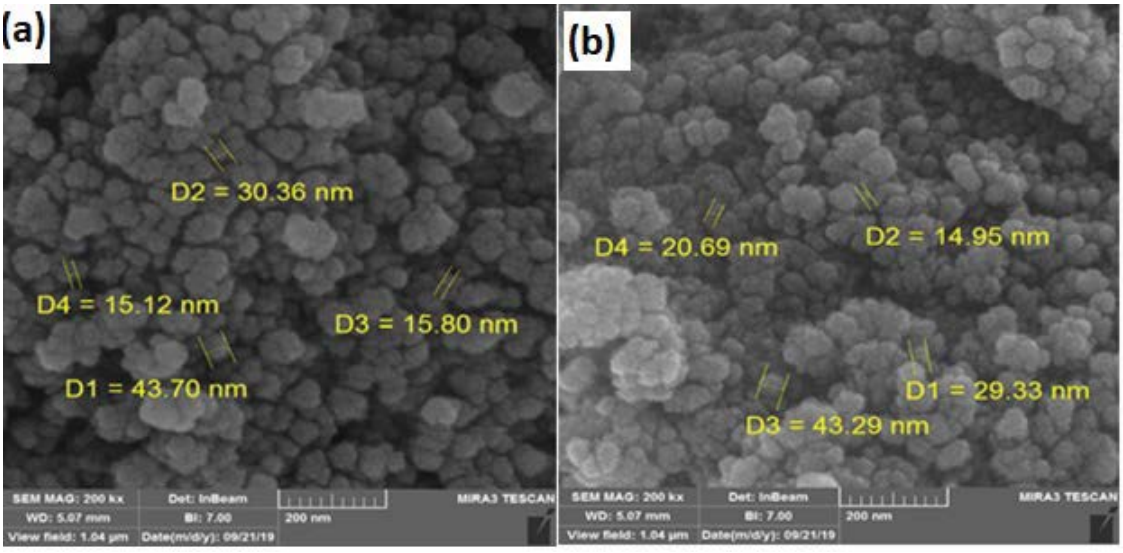

Fig. 9. Scanning electron microscopy images of the adsorbent surface. (a) Iron oxide(II) and (b) scallop shell/iron oxide(II) nanocomposite.

3.7. Kinetics study of DR81 adsorption

According to the removal values of DR81 in the mentioned contact times, the first and second-order kinetics of the adsorption process were calculated, and the results of the calculations of the kinetic parameters of DR81 adsorption by scallop shell/iron oxide(II) nanocomposite are presented in Table 3. According to this table, dye adsorption by scallop shell/iron oxide(II) nanocomposite shows a high correlation with pseudo-second-order kinetics. Also, adsorption kinetics studies were studied at different concentrations. Also, the experimental data obtained from the experiments were more correlated and consistent with the pseudo-second-order kinetic model. The correlation coefficient related to the pseudo-second-order kinetics for all concentrations was higher than the correlation coefficient of the pseudo-first-order model.

Analysis of information obtained from isotherms is very important to develop an equation by which the necessary design can be done. In addition, the adsorption isotherm can be used to describe how the adsorbent and adsorbent react as well as to optimize the amount of adsorbent used [9]. Based on the results of isothermal studies, the correlation coefficient of the Langmuir isotherm equation shows the best interpretation of DR81 adsorption by scallop shell/iron oxide nanocomposite [48]. In a study conducted by Ashrafi et al. [10] for the adsorption of DR81 and methylene blue dyes with modified rice husk/NaOH from aqueous solutions, the results showed that the maximum adsorption capacity was 6 mg/g. In order to obtain information about the factors affecting the reaction rate, it is necessary to evaluate the adsorption kinetics. R^2 values of the pseudo-first-order and second-order kinetics based on the results of the study of DR81 absorption kinetics in Table 3 are equal to 0.89 and 0.995, respectively, which indicates the obedience of our studied adsorption process from the pseudo-second-order kinetic. Although the predominant process in adsorption of DR81 is the physical type, the presence of a small amount of chemical adsorption can be the main factor in rate control in this study.

The value of q_m for this study was 46.4 mg/g, which to be higher than several adsorbent employed in recent studies conducted for DR81 adsorption at their experimental conditions (Table 4), confirming the advantage and efficiency of this work.

3.8. Study of thermodynamic parameters for DR81 adsorption

To investigate the thermodynamic parameter, the adsorption process was conducted under optimal conditions (pH of 3, adsorbent value of 0.5 g/L, DR81 concentration of 25 mg/L, and temperatures of 25°C–55°C) for 120 min and then the DR81 concentration and the residue in the solution were determined. According to the results, the process efficiency decreased with increasing temperature. The results related to thermodynamic parameters were presented in Table 5.

3.9. Effect of interfering ions on DR81 adsorption

In this study, interfering ions such as KCl, KH_2PO_4, Na_2CO_3 and $NaNO_3$ were used to evaluate the effect of interfering anions and cations on the DR81 adsorption process. For this purpose, concentrations of 0.5 M of KCl, KH_2PO_4, Na_2CO_3 and $NaNO_3$ at a DR81concentration of 25 mg/L, adsorbent dose of 2 g/L were examined at a pH of 3 (Fig. 10). As can be seen, when distilled water was used, the mean removal of DR81 was 98%, while presence of interfering ions reduced the removal of DR81 using the scallop shell/iron oxide(II) adsorbent. The removal efficiency were 96.3,

Table 4
Comparison of the adsorption of Direct red 81 by scallop shell/iron oxide nanocomposite and other reported adsorbents

Adsorbent	q_m (mg/g)	References
Scallop shell/ iron oxide	46.2	This work
Kaolinite	26.5	[42]
Treated bamboo sawdust	13.83	[9]
Bamboo sawdust	6.4	[9]
Magnesium oxide-coated kaolinite (Mg-Kaol)	55.7	[42]
Iron filings	25.3	[49]
Balsamodendron caudatum wood	147	[50]
Chamomilla plant	10.1	[51]
Modified silk maze	55	[51]

Table 5
Thermodynamic parameters of Direct red 81 adsorption

T (K)	ΔG (kJ/mol)	ΔH (kJ/mol)	ΔS (J/mol·K)
298.15	–1.29	–2.3	0.92
308.15	–1.751		
308.15	–1.93		
328.15	–2.7		

Table 3
Calculated parameters for Direct red 81 adsorption

Initial concentration of dye (mg/L)	Pseudo-first-order			Pseudo-second-order			
	R^2	k_1 (min^{-1})	$q_{e,cal}$ (mg/g)	R^2	k_2 (g/mg·min)	$q_{e,cal}$ (mg/g)	$q_{e,exp}$ (mg/g)
25	0.48	0.0191	12.28	0.998	0.01	3.72	12.29
50	0.89	0.05	18.54	0.995	0.07	7.66	20.38
75	0.91	0.006	26.3	0.99	0.03	12.6	27.15
100	0.85	0.008	19.1	0.99	0.02	53.2	20.2

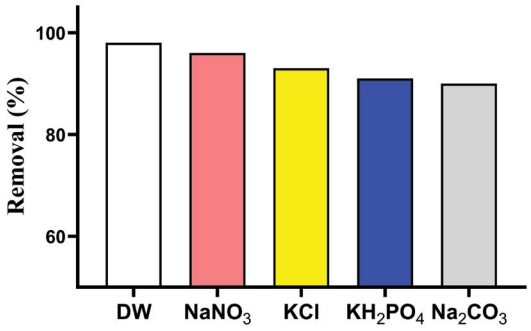

Fig. 10. Effect of interfering ions (0.5 M) on Direct red 81 adsorption (Direct red 81 concentration 25 mg/L, adsorbent dosage of 2 g/L, time of reaction 90 min and pH of 3).

93.1, 91.5 and 90.8% in the presence of 0.5 M of $NaNO_3$, KCl, KH_2PO_4 and Na_2CO_3, respectively. The results show that the anions and cations in the solution do not have a significant effect on the adsorption efficiency DR81 onto the scallop shell/iron oxide(II) adsorbent.

4. Conclusion

The results showed that the DR81 adsorption on the nanocomposite followed the Langmuir isotherm (R^2 = 0.996), and the results of the kinetic equations also showed that the DR81 adsorption behavior per unit time obeys the pseudo-second-order kinetic model (R^2 = 0.995). The maximum adsorption coefficient was 46.4 mg/g. The thermodynamic parameters showed that the adsorption of DR81 on the iron oxide/scallop shell adsorbent is exothermic and spontaneous. According to the results, iron oxide/scallop shell nanocomposite can be used as a cheap adsorbent with good efficiency for adsorption of DR81 compared to other natural adsorbents.

Acknowledgements

This article was extracted from the Master's Thesis in Environmental Health Engineering at Guilan University of Medical Sciences and Health Services with a project code number: 72603 and code of ethics committee IR. GUMS. REC.1400.372. The authors appreciate the officials of the Deputy of Research for their financial support and the experts of the Environmental Health Laboratories of the Faculty of Health who have assisted in the implementation of this research.

References

[1] J. Jaafari, A.B. Javid, H. Barzanouni, A. Younesi, N.A.A. Farahani, M. Mousazadeh, P. Soleimani, Performance of modified one-stage Phoredox reactor with hydraulic up-flow in biological removal of phosphorus from municipal wastewater, Desal. Water Treat., 171 (2019) 216–222.
[2] J. Jaafari, K. Yaghmaeian, Response surface methodological approach for optimizing heavy metal biosorption by the blue-green alga *Chroococcus disperses*, Desal. Water Treat., 142 (2019) 225–234.
[3] D. Naghipour, K. Taghavi, M. Ashournia, J. Jaafari, R. Arjmand Movarrekh, A study of Cr(VI) and NH_4^+ adsorption using greensand (glauconite) as a low-cost adsorbent from aqueous solutions, Water Environ. J., 34 (2020) 45–56.
[4] D. Naghipour, E. Rouhbakhsh, J. Jaafari, Application of the biological reactor with fixed media (IFAS) for removal of organic matter and nutrients in small communities, Int. J. Environ. Anal. Chem., 102 (2022) 5811–5821.
[5] D. Naghipour, L. Hoseinzadeh, K. Taghavi, J. Jaafari, Characterization, kinetic, thermodynamic and isotherm data for diclofenac removal from aqueous solution by activated carbon derived from pine tree, Data Brief, 18 (2018) 1082–1087.
[6] S.Z. Ghazanfari, J. Jaafari, S.D. Ashrafi, K. Taghavi, Decolourisation of Direct red dye 81 from aqueous solutions by SnO_2/H_2O_2 hybrid process, Int. J. Environ. Anal. Chem., (2021) 1–15, doi: 10.1080/03067319.2021.1921758.
[7] W. Li, Z. Xie, S. Xue, H. Ye, M. Liu, W. Shi, Y. Liu, Studies on the adsorption of dyes, Methylene blue, Safranin T, and Malachite green onto polystyrene foam, Sep. Purif. Technol., 276 (2021) 119435, doi: 10.1016/j.seppur.2021.119435.
[8] E. Walger, N. Marlin, F. Molton, G. Mortha, Study of the Direct red 81 dye/copper(II)-phenanthroline system, Molecules, 23 (2018) 242, doi: 10.3390/molecules23020242.
[9] A. İmran, S. Dahiya, K. Tabrez, Removal of Direct red 81 dye from aqueous solution by native and citric acid modified bamboo sawdust—kinetic study and equilibrium isotherm analyses, Gazi Univ. J. Sci., 25 (2012) 59–87.
[10] S. Ashrafi, H. Kamani, A. Mahvi, The optimization study of Direct red 81 and Methylene blue adsorption on NaOH-modified rice husk, Desal. Water Treat., 57 (2016) 738–746.
[11] M. Rouhani, S.D. Ashrafi, K. Taghavi, M.N. Joubani, J. Jaafari, Evaluation of tetracycline removal by adsorption method using magnetic iron oxide nanoparticles (Fe_3O_4) and clinoptilolite from aqueous solutions, J. Mol. Liq., 356 (2022) 119040, doi: 10.1016/j.molliq.2022.119040.
[12] H. Faraji, A.A. Mohamadi, H.R. Soheil Arezomand, A.H. Mahvi, Kinetics and equilibrium studies of the removal of Blue basic 41 and Methylene blue from aqueous solution using rice stems, Iran. J. Chem. Chem. Eng. (IJCCE), 34 (2015) 33–42.
[13] J. Lin, W. Ye, H. Zeng, H. Yang, J. Shen, S. Darvishmanesh, P. Luis, A. Sotto, B. van der Bruggen, Fractionation of direct dyes and salts in aqueous solution using loose nanofiltration membranes, J. Membr. Sci., 477 (2015) 183–193.
[14] S. Zodi, B. Merzouk, O. Potier, F. Lapicque, J.-P. Leclerc, Direct red 81 dye removal by a continuous flow electrocoagulation/flotation reactor, Sep. Purif. Technol., 108 (2013) 215–222.
[15] M. Yekrangi, M.K. Mohammadi, A. Doulah, Investigation and optimization of removal of reactive red and reactive blue dyes existing in cane sugar wastewater, entrance to Shadegan wetland with chitosan absorbent, J. Wetland Ecobiol., 11 (2019) 39–50.
[16] A. Deb, A. Debnath, B. Saha, Ultrasound-aided rapid and enhanced adsorption of anionic dyes from binary dye matrix onto novel hematite/polyaniline nanocomposite: response surface methodology optimization, Appl. Organomet. Chem., 34 (2020) e5353, doi: 10.1002/aoc.5353.
[17] A. Deb, M. Kanmani, A. Debnath, K.L. Bhowmik, B. Saha, Ultrasonic assisted enhanced adsorption of methyl orange dye onto polyaniline impregnated zinc oxide nano.: kinetic, isotherm and optimization of process parameters, Ultrason. Sonochem., 54 (2019) 290–301.
[18] A. Deb, A. Debnath, B. Saha, Sono-assisted enhanced adsorption of Eriochrome Black-T dye onto a novel polymeric nanocomposite: kinetic, isotherm, and response surface methodology optimization, J. Dispersion Sci. Technol., 42 (2021) 1579–1592.
[19] H. Soleimani, A.H. Mahvi, K. Yaghmaeian, A. Abbasnia, K. Sharafi, M. Alimohammadi, M. Zamanzadeh, Effect of modification by five different acids on pumice stone as natural and low-cost adsorbent for removal of humic acid from aqueous solutions - application of response surface methodology, J. Mol. Liq., 290 (2019) 111181, doi: 10.1016/j.molliq.2019.111181.
[20] M. Moradi, A.M. Mansouri, N. Azizi, J. Amini, K. Karimi, K. Sharafi, Adsorptive removal of phenol from aqueous solutions by copper (Cu)-modified scoria powder: process modeling and kinetic evaluation, Desal. Water Treat., 57 (2016) 11820–11834.

[21] C. Tizaoui, N. Grima, Kinetics of the ozone oxidation of Reactive Orange 16 azo-dye in aqueous solution, Chem. Eng. J., 173 (2011) 463–473.
[22] H.N. Saleh, M.H. Dehghani, R. Nabizadeh, A.H. Mahvi, F. Hossein, M. Ghaderpoori, M. Yousefi, A. Mohammadi, Data on the Acid black 1 dye adsorption from aqueous solutions by low-cost adsorbent- *Cerastoderma lamarcki* shell collected from the northern coast of Caspian Sea, Data Brief, 17 (2018) 774–780.
[23] D. Naghipour, K. Taghavi, J. Jaafari, I. Kabdaşlı, M. Makkiabadi, M. Javan Mahjoub Doust, F. Javan Mahjoub Doust, Scallop shell coated Fe_2O_3 nanocomposite as an eco-friendly adsorbent for tetracycline removal, Environ. Technol., 44 (2023) 150–160, doi: 10.1080/09593330.2021.1966105.
[24] M. Shirzad-Siboni, A. Mohagheghian, R. Vahidi-Kolur, M. Pourmohseni, J.-K. Yang, Preparation and characterization of scallop shell coated with Fe_3O_4 nanoparticles for the removal of azo dye: kinetic, equilibrium and thermodynamic studies, Indian J. Chem. Technol. (IJCT), 25 (2018) 40–50.
[25] S. Khamparia, D. Jaspal, Adsorptive removal of Direct red 81 dye from aqueous solution onto *Argemone mexicana*, Sustainable Environ. Res., 26 (2016) 117–123.
[26] Z.-G. Wu, Y. Wang, One-pot synthesis of magnetic γ-Fe_2O_3 nanoparticles in ethanol-water mixed solvent, Mater. Sci.-Pol., 31 (2013) 577–580.
[27] R. Shokoohi, M. Salari, M. Molla Mahmoudi, S. Azizi, S.A. Ghiasian, J. Faradmal, H. Faraji, The sorption of cationic and anionic heavy metal species on the biosorbent of *Aspergillus terreus*: isotherm, kinetics studies, Environ. Prog. Sustainable Energy, 39 (2020) e13309, doi: 10.1002/ep.13309.
[28] D. Naghipour, L. Hoseinzadeh, K. Taghavi, J. Jaafari, A. Amouei, Effective removal of tetracycline from aqueous solution using biochar prepared from pine bark: isotherms, kinetics and thermodynamic analyses, Int. J. Environ. Anal. Chem., (2021) 1–14, doi: 10.1080/03067319.2021.1942462.
[29] M.-A. Zazouli, D. Balarak, Y. Mahdavi, Effect of *Azolla filiculoides* on removal of Reactive red 198 in aqueous solution, J. Adv. Environ. Health Res., 1 (2013) 44–50.
[30] M. Moradi, M. Soltanian, M. Pirsaheb, K. Sharafi, S. Soltanian, A. Mozafari, The efficiency study of pumice powder to lead removal from the aquatic environment: isotherms and kinetics of the reaction, J. Mazandaran Univ. Med. Sci., 22 (2013) 65–75.
[31] Y. Mahdavi, F. Ghorzin, S. Sadeghi, Biosorption of Acid blue 113 dyes using dried *Lemna minor* biomass, Sci. J. Environ. Sci., 5 (2016) 152–158.
[32] L. Wang, J. Li, Adsorption of C.I. Reactive red 228 dye from aqueous solution by modified cellulose from flax shive: kinetics, equilibrium, and thermodynamics, Ind. Crops Prod., 42 (2013) 153–158.
[33] S. Chatterjee, S. Chatterjee, B.P. Chatterjee, A.K. Guha, Adsorptive removal of Congo red, a carcinogenic textile dye by chitosan hydrobeads: binding mechanism, equilibrium and kinetics, Colloids Surf., A, 299 (2007) 146–152.
[34] M. Erşan, Removal of tetracycline using new biocomposites from aqueous solutions, Desal. Water Treat., 57 (2016) 9982–9992.
[35] M.A. Zazouli, A.H. Mahvi, S. Dobaradaran, M. Barafrash-tehpour, Y. Mahdavi, D. Balarak, Adsorption of fluoride from aqueous solution by modified *Azolla filiculoides*, Adsorption, 47 (2014) 349–358.
[36] B. Rouhi Broujeni, A. Nilchi, A.H. Hassani, R. Saberi, Preparation and characterization of chitosan/Fe_2O_3 nano composite for the adsorption of thorium(IV) ion from aqueous solution, Water Sci. Technol., 78 (2018) 708–720.
[37] S. Shams, A.U. Khan, Q. Yuan, W. Ahmad, Y. Wei, Z. Ul Haq Khan, S. Shams, A. Ahmad, A. Ur Rahman, S. Ullah, Facile and eco-benign synthesis of Au@Fe_2O_3 nanocomposite: efficient photocatalytic, antibacterial and antioxidant agent, J. Photochem. Photobiol., B, 199 (2019) 111632, doi: 10.1016/j.jphotobiol.2019.111632.
[38] S.E. Gerami, M. Pourmadadi, H. Fatoorehchi, F. Yazdian, H. Rashedi, M.N. Nigjeh, Preparation of pH-sensitive chitosan/polyvinylpyrrolidone/α-Fe_2O_3 nanocomposite for drug delivery application: emphasis on ameliorating restrictions, Int. J. Biol. Macromol., 173 (2021) 409–420.
[39] M. Dehghani, M. Ansari Shiri, S. Shahsavani, N. Shamsedini, M. Nozari, Removal of Direct red 81 dye from aqueous solution using neutral soil containing copper, Desal. Water Treat., 86 (2017) 213–220.
[40] A. Fakhri, Utilization of tungsten trioxide nanoparticles and nickel oxide pillared montmorillonite nanocomposites for the adsorption of the drug dexamethasone from aqueous solutions, RSC Adv., 5 (2015) 22199–22208.
[41] M. Vadi, N. Hossinie, Z. Shekari, Comparative study of adsorption isotherms steroidal anti-inflammatory drug dexamethasone on carbon nanotube and activated carbon, Orient. J. Chem., 29 (2013) 491–496.
[42] T.A. Khan, S. Dahiya, E.A. Khan, Removal of Direct red 81 from aqueous solution by adsorption onto magnesium oxide-coated kaolinite: isotherm, dynamics and thermodynamic studies, Environ. Prog. Sustainable Energy, 36 (2017) 45–58.
[43] M.T. Ghaneian, M. Dehvari, M. Taghavi, M. Amrollahi, B. Jamshidi, Application of pomegranate seed powder in the removal of Reactive red 198 dye from aqueous solutions, Jundishapur J. Health Sci., 4 (2012) e93988.
[44] J. Zhang, X. Liu, L. Wang, T. Yang, X. Guo, S. Wu, S. Wang, S. Zhang, Synthesis and gas sensing properties of α-Fe_2O_3@ZnO core–shell nanospindles, Nanotechnology, 22 (2011) 185501, doi: 10.1088/0957-4484/22/18/185501.
[45] J. Zang, T. Wu, H. Song, N. Zhou, S. Fan, Z. Xie, J. Tang, Removal of tetracycline by hydrous ferric oxide: adsorption kinetics, isotherms, and mechanism, Int. J. Environ. Anal. Chem., 16 (2019) 4580, doi: 10.3390/ijerph16224580.
[46] S. Shojaei, S. Shojaei, M. Sasani, The efficiency of eliminating Direct red 81 by zero-valent iron nanoparticles from aqueous solutions using response surface model (RSM), Model. Earth Syst. Environ., 3 (2017) 1–7, doi: 10.1007/s40808-017-0287-y.
[47] M. Arami, N.Y. Limaee, N.M. Mahmoodi, N.S. Tabrizi, Equilibrium and kinetics studies for the adsorption of direct and acid dyes from aqueous solution by soy meal hull, J. Hazard. Mater., 135 (2006) 171–179.
[48] M.M. Alam, M.W. Murad, A.H.M. Noman, I. Ozturk, Relationships among carbon emissions, economic growth, energy consumption and population growth: testing environmental Kuznets curve hypothesis for Brazil, China, India and Indonesia, Ecol. Indic., 70 (2016) 466–479.
[49] M. Dehghani, M. Nozari, A. Fakhraei Fard, M. Ansari Shiri, N. Shamsedini, Direct red 81 adsorption on iron filings from aqueous solutions; kinetic and isotherm studies, Environ. Technol., 40 (2019) 1705–1713.
[50] B. Sivakumar, P. Nithya, S. Karthikeyan, C. Kannan, Kinetics, equilibrium and isotherms of Direct red 81 removal from aqueous solution using *Balsamodendron caudatum* wood waste activated nanoporous carbon, Rasayan J. Chem., 7 (2014) 161–169.
[51] H.M. Momen, P. Ardalan, A. Vafaie, Equilibrium and kinetic studies of Direct red 81 biosorption onto modified silk maze as an economical biosorbent, J. Chem. Health Risks, 4 (2014), doi: 10.22034/JCHR.2018.544058.